Naval Research Laboratory

Washington, DC 20375-5320

NRL/MR/6180--20-10,186

Spontaneous Raman Scattering Measurements in the Exhaust Plume of a Micro-Thruster Nozzle Operated in a Low-Pressure Environment

Aaron W. Skiba

Former ASEE Postdoctoral Fellow
Washington, DC

Brian T. Fisher

Combustion and Reacting Transport Section
Chemistry Division

Alfredo D. Tuesta

Former NRL employee

Logan T. Williams
Michael F. Osborn

Propulsion Section
Spacecraft Engineering Department

November 17, 2020

REPORT DOCUMENTATION PAGE

Form Approved
OMB No. 0704-0188

1. REPORT DATE *(DD-MM-YYYY)*	**2. REPORT TYPE**	**3. DATES COVERED** *(From - To)*
17-11-2020	NRL Memorandum Report	April 2019 – July 2020

4. TITLE AND SUBTITLE

Spontaneous Raman Scattering Measurements in the Exhaust Plume of a Micro-Thruster Nozzle Operated in a Low-Pressure Environment

5a. CONTRACT NUMBER

5b. GRANT NUMBER

5c. PROGRAM ELEMENT NUMBER

6. AUTHOR(S)

Aaron W. Skiba*, Brian T. Fisher, Alfredo D. Tuesta**, Logan T. Williams, and Michael F. Osborn

5d. PROJECT NUMBER

5e. TASK NUMBER

5f. WORK UNIT NUMBER
6A29

7. PERFORMING ORGANIZATION NAME(S) AND ADDRESS(ES)

Naval Research Laboratory
4555 Overlook Avenue, SW
Washington, DC 20375-5320

8. PERFORMING ORGANIZATION REPORT NUMBER

NRL/MR/6180--20-10,186

9. SPONSORING / MONITORING AGENCY NAME(S) AND ADDRESS(ES)

Naval Research Laboratory
4555 Overlook Avenue, SW
Washington, DC 20375-5320

10. SPONSOR / MONITOR'S ACRONYM(S)

NRL BASE 6.2

11. SPONSOR / MONITOR'S REPORT NUMBER(S)

12. DISTRIBUTION / AVAILABILITY STATEMENT

DISTRIBUTION STATEMENT A: Approved for public release; distribution is unlimited.

13. SUPPLEMENTARY NOTES

*Former American Society of Engineering Education (ASEE) Postdoctoral Fellow
**Former employee

14. ABSTRACT

Measurements of spontaneous Raman scattering signals made within the exhaust plume of a micro-nozzle are reported and discussed. The measurements used a novel fiber-coupled, multiple-pass cell, spontaneous Raman scattering spectroscopy system, which was designed to measure H2 rotational Raman transitions within low-pressure environments void of optical access. When signal to noise ratios permit it, theoretical spectra can be fit to the results to yield temperature measurements. At low pressures, the number densities in the exhaust of a micro-nozzle operating in a high-vacuum environment are prohibitively low, rendering such measurements extraordinarily challenging. Methods to improve the quality of the measurements are discussed and contrasted in terms of the spatial resolution they offer. This work provides insights into the limitations of these non-intrusive measurements within the exhaust plume of a micro-nozzle and establishes a roadmap for improving their quality.

15. SUBJECT TERMS

Raman spectroscopy Multiple-pass cell Low pressure spectroscopy
Microjet Resistojet

16. SECURITY CLASSIFICATION OF:			**17. LIMITATION OF ABSTRACT**	**18. NUMBER OF PAGES**	**19a. NAME OF RESPONSIBLE PERSON**
a. REPORT	**b. ABSTRACT**	**c. THIS PAGE**			Brian T. Fisher
Unclassified Unlimited	Unclassified Unlimited	Unclassified Unlimited	Unclassified Unlimited	20	**19b. TELEPHONE NUMBER** *(include area code)* (202) 404-3365

Standard Form 298 (Rev. 8-98)
Prescribed by ANSI Std. Z39.18

This page intentionally left blank.

CONTENTS

FIGURES

SPONTANEOUS RAMAN SCATTERING MEASUREMENTS IN THE EXHAUST PLUME OF A MICRO-THRUSTER NOZZLE OPERATED IN A LOW-PRESSURE ENVIRONMENT

INTRODUCTION

In an effort to reduce the cost of deploying satellites in space, there has been a trend towards minimizing their size. For instance, numerous CubeSats, which are typically only $(100 \times 100 \times 300)$ mm^3 in size, are now in orbit around the Earth. Due to their small size, such satellites typically lack thrusters capable of allowing them to maneuver, which significantly restricts their lifespan. A micro-resistojet thruster has been proposed as a means to increase the lifespan and versatility of CubeSats [1-4]. A micro-resistojet works by resistively heating a gas and expanding it through a micro-nozzle, which can have throat and exit-plane diameters on the order of ~150 μm and ~1 mm, respectively [1-4]. The small length scales of these nozzles coupled with the low flow rates that pass through them lead to them operating in a low Reynolds number (*Re*) regime. As such, viscous effects and boundary layer development within these nozzles have a large influence on their performance [5]. Understanding this influence is critical to the design of efficient micro-nozzles intended for use with micro-resistojet thrusters.

Numerous computational simulations have been performed to understand the effects of viscous boundary layer development on the performance of micro-thruster nozzles [6-14]. The fidelity of such simulations is, however, contingent on the ability of their results to replicate those from experimental measurements. Moreover, the predictive capabilities of such numerical models often require accurate knowledge of the boundary conditions associated with a particular thruster. To guide the development of predictive models and to provide results for comparisons to those they produce, multiple experiments have performed at the U.S. Naval Research Laboratory (NRL) to measure the performance of resistojet thrusters under relevant conditions [3, 4]. Additionally, several studies at other institutions investigated the thermodynamic properties of the flows within and issuing from resistojet thrusters [7, 14, 15]. Laser-based measurements, which included Coherent Anti-Stokes Raman Spectroscopy (CARS) and spontaneous Raman scattering, were utilized in the latter experiments to measure the temperature of and concentrations of species within the flows of resistojet thrusters operated in low-pressure environments [7, 14, 15]. The thrusters considered in those studies were, however, much larger than those intended for use on CubeSats. Those thrusters operated in a higher *Re* regime and were not as susceptible to the influences of viscous boundary layer development. Therefore, to increase understanding of the boundary layer, an integrated program was conducted to experimentally measure and numerically simulate nozzle performance. In order to develop numerical tools that accurately and efficiently simulate flows through micro-nozzles, there is a need to measure the thermodynamic properties of their exhaust plumes while operating in near-vacuum environments.

OBJECTIVE

The primary objective of this study is to demonstrate the use of a novel fiber-coupled, multiple-pass cell (MPC), spontaneous Raman scattering spectroscopy system to measure rotational Raman signals from H_2 issuing from a micro-thruster operated within a vacuum chamber. While this system was successfully employed in a quiescent vacuum chamber, the detection of useful Raman measurements proved elusive. Thus, a secondary objective of this work is to understand issues and challenges hindering such measurements. The results of this secondary objective serve to determine how to improve the spectroscopy system to ensure successful measurements in future efforts.

Manuscript approved November 6, 2020.

EXPERIMENT

This section provides details pertaining to the experiment and its individual systems. First the micro-nozzle and the chamber it is operated in are described. Then details pertaining to the diagnostic system employed in this study are provided. Finally, a description of the procedure implemented to reduce and analyze the collected data is outlined at the end of this section.

Micro-nozzle and vacuum chamber

The experiments were conducted within a vacuum chamber at NRL, which complement those performed previously [3, 4]. This chamber measures 2 m in diameter and is 2.3 m tall. The chamber is pumped down via a 1.2 m NRC diffusion pump with a nominal pumping speed of 100,000 l/s for air. A Leybold WH2500 blower and a SV-630B roughing pump, with a combined pumping speed of 4.3×10^4 liters per minute, are also employed to support the diffusion pump. The combined use of these pumps enables base operating pressures of 5.5×10^{-6} Torr (i.e. ~1 mPa) within the chamber. At rough vacuum conditions, a Granville Phillips 275 convectron gauge is used for pressure monitoring, while at high vacuum, a Bayard-Alpert type ion gauge is used.

The micro-thruster nozzle considered in this study was mounted to a specialized thrust stand within the aforementioned vacuum chamber. The nozzle is comprised of a stainless-steel casing with welded Swagelok fitting adaptors for a gas feed line, a thermocouple, a pressure transducer, and a cartridge heater. The gas is introduced at the back end of the nozzle assembly, is then forced through the heating elements, and is finally ejected out the nozzle. In this study, a single nozzle was considered, which has a throat diameter of 0.152 mm, a cone half-angle of 30°, and an exit diameter of 1.52 mm. This nozzle was machined into a hexagonal nut with threads such that it could be secured to the assembly and easily replaced when needed. Details of the nozzle assembly and the nozzle itself used in these laboratory experiments are shown in Fig. 1 and Fig. 2, respectively.

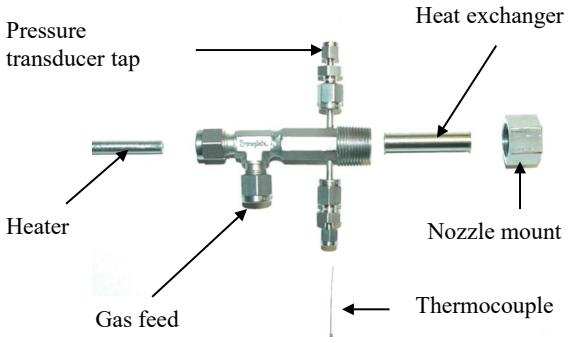

Fig. 1 Nozzle assembly used in laboratory-scale resistojet experiments.

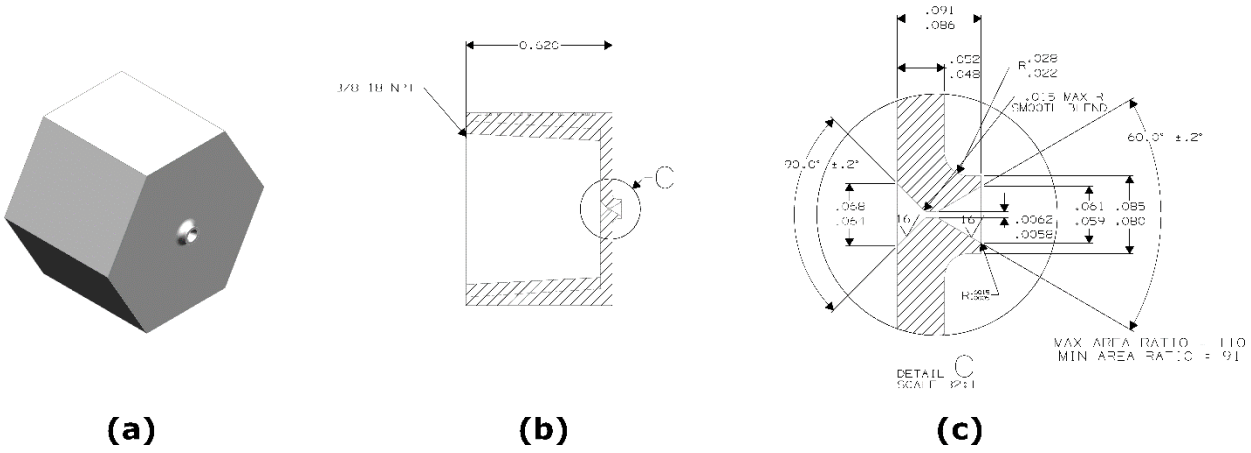

Fig. 2 Details of nozzle used in laboratory-scale resistojet experiments, including: (a) 3D drawing; (b) cross-section; and (c) nozzle dimensions.

Spontaneous Raman Scattering system

In this study, spontaneous Raman scattering measurements were facilitated by a novel fiber-coupled, multiple-pass cell (MPC), spontaneous Raman scattering spectroscopy system. A detailed description of this system is provided elsewhere [16], thus only a brief overview its primary components is provided here. This system consists of five major components. The first is a continuous wave (cw), solid-state laser (Coherent Verdi G5 Series SLM) that outputs 5 W of radiation at 532 nm. The second is a set of vacuum-compatible optical fibers that were produced by NKT Photonics. To introduce these fibers into the vaccum chamber, they were fed through two separate custom vacuum-feedthroughs (one for the laser-delivery fiber and one for that to return the signal to the spectrograph) that were assembled by Coastal Connections. One fiber transmits the high-power beam to the test section while the other relays the collected Raman signal to a spectrograph. The third component is the MPC (designed and fabricated by Southwest Sciences Inc.) [17, 18], which represents a modified Herriott cell [19, 20] and has the potential to amplify the Raman signal by a factor of ~100. A high-throughput (f/1.8) spectrograph (HoloSpec) is the fourth key piece of this system. This spectrograph was outfitted with a low-frequency holographic grating intended for use near 532 nm (HSG-532-LF) and long-pass filter (HS-HSPF-532.0), which served to attenuate light from Rayleigh and Mie scattering. The final component of this system is a low-noise, thermoelectrically cooled EMCCD camera (Andor Newton 920). To enhance the signal-to-noise ratio (SNR), multiple frames (two to ten) with exposure times between two and thirty minutes were collected for each measurement point. The combination of these separate components yields a compact, versatile, and highly sensitive Raman spectroscopy system that can be utilized in environments void of optical access (e.g., a large-scale vacuum chamber).

To obtain Raman measurements at multiple points within the exhaust plume from the micro-nozzle, the MPC was secured to a remote-controlled, 3-axis traverse system. As shown in Fig. 3a, the traverse system was mounted to the same isolation stage as the micro-thruster nozzle. A close-up, top-down image of the micro-nozzle and the MPC in operation in shown in Fig. 3b, which highlights the relative positioning of the probe volume with respect to the nozzle. As indicated in the lower left corner of this image, here the axes are such that *y* is positive out of the plane of the image, *z* is positive in the direction moving away from the nozzle, and *x* is positive to the right (from a top-down view). As is clearly seen in the image of the back mirror of the MPC in Fig. 3c, the probe volume embodies an elliptical pattern that is comprised of ~100 individual beams that reflect within the MPC.

Two separate orientations of the MPC were utilized in this study. The first is a horizontal orientation, which is depicted in Figs. 3c and 3d. In this orientation, the major axis of the elliptical probe volume is aligned with the flow issuing from the nozzle and is perpendicular to the collection optics (see Fig. 3a). The sketch in Fig. 3d serves to illustrate this configuration. Here, the out-of-plane resolution of the measurements is dictated by the minor axis of the probe volume, which can be minimized to ~180 μm (i.e. twice the beam thickness). The in-plane resolution is then set by the collection optics and any physical apertures included with them (this is illustrated by the shaded blue region in Fig. 3d) [16]. When no aperture is included in the collection system, it collects light from a region that is ~320 μm in diameter. By adding smaller diameter pinholes at the focal point of the collection optics, this region can be reduced to a diameter on the order of 1 μm. However, reducing the in-plane resolution also reduces the signal since a smaller aperture allows less light though to the detector.

The second orientation of the MPC utilized in this study was a vertical one obtained by rotating the horizontal orientation by 90°. In this configuration, which is depicted in Figs. 3e and 3f, the major axis of the probe volume is perpendicular to the flow. The advantage of this orientation is that it can provide the highest collected signal levels, since each pass of the laser (of which there are ~100) within the cell can contribute (consider the shaded blue region in Fig. 3f). The drawback to operating with this orientation is, however, that it offers the poorest resolution. Namely, for this configuration the resolution is set by the major axis of the probe volume, which is ~1-mm long. Yet, one additional advantage this configuration has over the horizontal configuration is that it allows the probe volume to be positioned very close (within 100s of microns) to the exit of the nozzle. In contrast, due to the focusing of beams within the MPC from a volume that is ~58 mm long on the mirrors to one that is ~1 mm long within distance of 100 mm, the probe volume cannot be placed within ~1 mm of the nozzle when operated in the horizontal configuration without portions of the reflected beams being clipped by the hexagon nut the nozzle is machined in (see Fig. 3b).

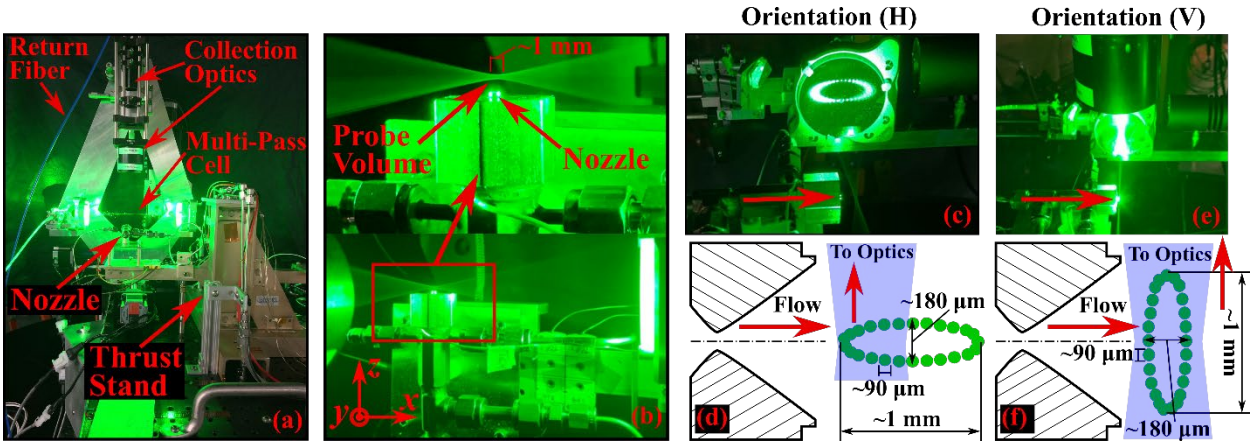

Fig. 3 Image depicting the Multiple-pass cell mounted on the test stand in (a) and a close-up of the micro-nozzle and the probe volume in (b). Panel (c) highlights the elliptical pattern traced by the laser beam as it reflects within the MPC. Panel (d) provides a sketch (not to scale) of the nozzle and probe volume.

Data processing

Each measurement was collected in an image format, like that shown in Fig. 4a. To extract one-dimensional (1-D) spectra from such images, background signal was first removed. Here, background signal is associated with the pixel offset of the camera and that which originates from reflected laser-light not fully rejected by the notch filter. An image of background signal is provided in Fig. 4b, which was obtained in presence of laser radiation but the absence of gas flow. Figure 4c presents the result of subtracting the background image from the measurement image. Following this subtraction, the images are

vertically integrated over the range of pixels between the magenta lines in Fig. 4c to produce a 1-D spectra like that in Fig. 4d.

The dotted black line in Fig. 4d corresponds to the raw data obtained from Fig. 4c, while the red line represents a filtered version of the raw data. Here, the data were subjected to 1-D wavelet-based filtering to increase their SNRs. When SNRs are sufficient, accurate temperature measurements can be obtained from the H_2 Raman spectra by fitting them with theoretical spectra [16, 21]. Figure 4e displays a best-fit theoretical spectrum (solid blue line) to the filtered data (dotted black line) in Fig 2d. In this case, the temperature providing the best fit is 290.6 K, which makes sense as these measurements were made with an unheated flow of H_2 issuing into the chamber. In this instance, relatively strong H_2 Raman signals were observed because a large, unmetered flow of H_2 was allowed into the chamber until its background pressure reached ~3.6 Torr. However, as will be evident from the following sections, conditions with much lower flow rates and operating pressures pose a significant challenge for facilitating accurate temperature measurements in the exhaust of a micro-thruster.

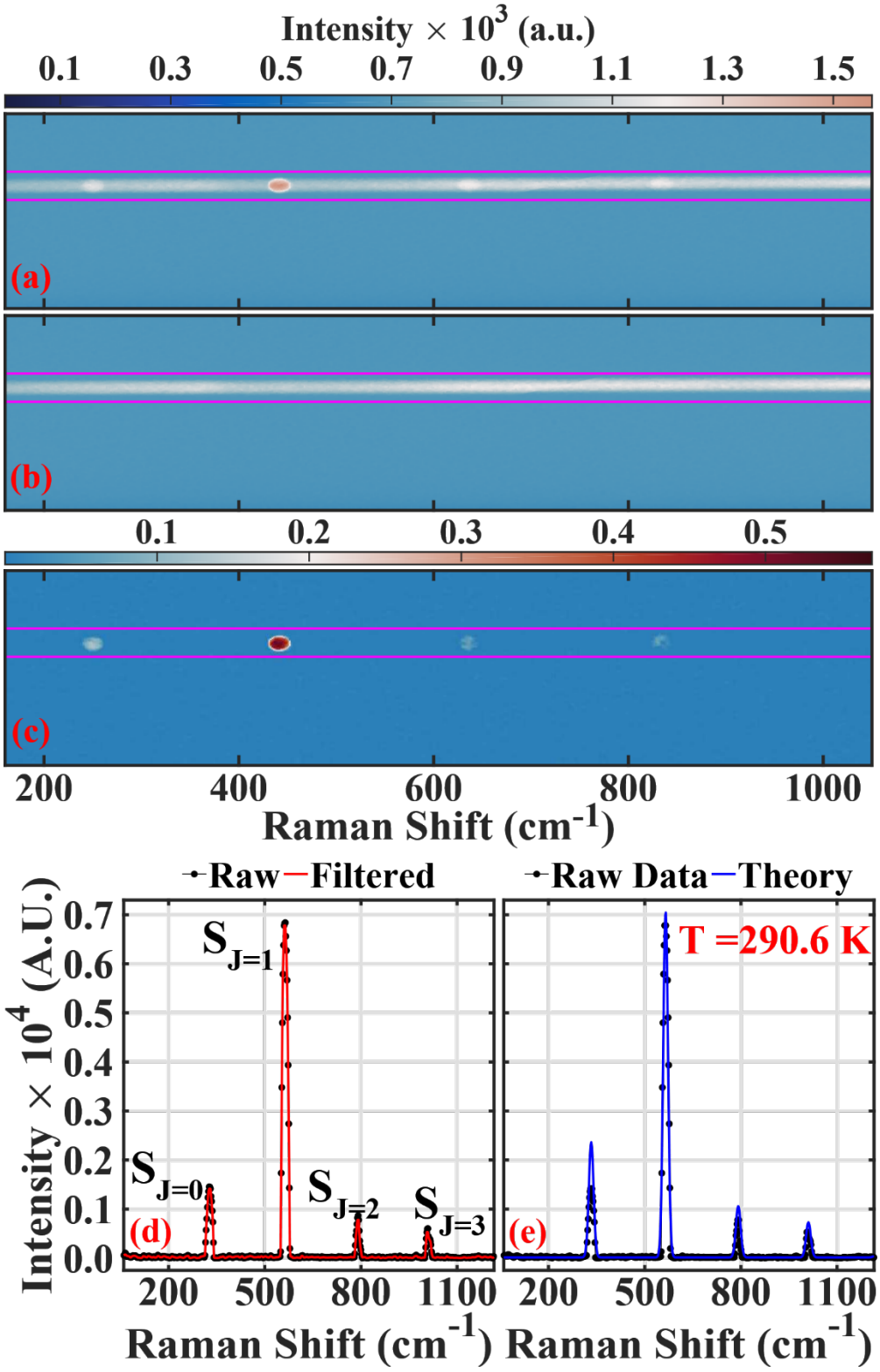

Fig. 4 Spectrum from measurements with large concentration of H_2 in the chamber at 3.6 Torr.

RESULTS

This section presents and discusses the results of spontaneous Raman measurements made within the vacuum chamber facility described above.

High-vacuum conditions

In this study, high-vacuum conditions correspond to chamber pressures between 3×10^{-5} Torr and 2×10^{-4} Torr. In contrast, Low-vacuum conditions are those with chamber pressers in the range of 0.02 Torr to 4 Torr. While the low-vacuum conditions do not represent a range in which micro-thrusters are meant to operate, they help highlight challenges associated with making successful Raman measurements under high-vacuum conditions.

Figure 5 presents spectra obtained under high-vacuum conditions. Specifically, Fig. 5 displays measurements made at three separate locations with a chamber pressure of 9.0×10^{-5} Torr, the MPC oriented horizontally, and with 600 sccm of H_2 flowing through the nozzle. Each spectrum in Fig. 5 represents the summation of background-corrected signal from 14 exposures, each with a collection time of 180 seconds. The vertical blue lines in Fig. 5 mark the expected locations of the first four H_2 rotational lines, yet, it is evident that no Raman signal was discernible in these measurements.

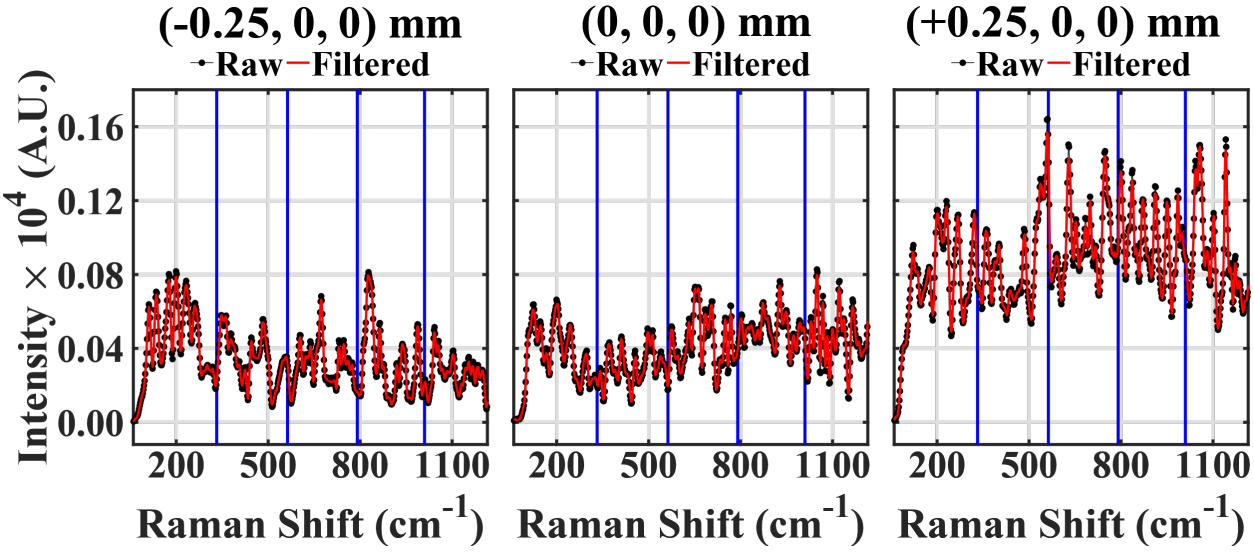

Fig. 5 High-vacuum measurements. The chamber pressure was ~9.0×10^{-5} Torr and the relative position of the probe volume is indicated above each panel as (x, y, z). Note, with the probe volume oriented horizontally, $z = 0$ corresponds to a location ~1 mm downstream of the nozzle exit. Each spectrum represents the sum of 14, 180-second long camera exposures.

In an attempt to increase the chances of observing a Raman signal, additional measurements were made with the probe volume oriented vertically (recall that significantly more passes contribute in this configuration) and with 1000 sccm of H_2 flowing through the nozzle. Results of such measurements are presented in Fig. 6, which displays spectra from three separate locations that were derived from two background-corrected, 600-second long exposures. Though even with the increased flow rate and enhanced signal offered by the vertical orientation of the probe volume, a Raman signal is not observed. (Note, the "spike" in the rightmost panel is just noise.)

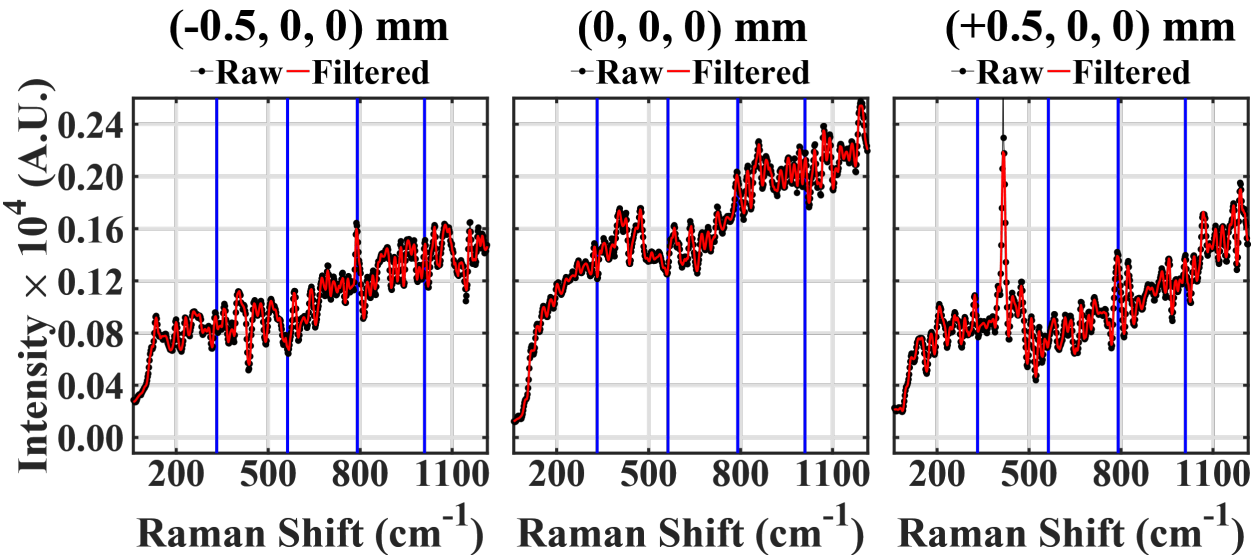

Fig. 6 High-vacuum measurements. The chamber pressure was ~1.1×10^{-4} Torr and the relative position of the probe volume is indicated above each panel as (x, y, z). Note, with the probe volume oriented vertically, $z = 0$ corresponds to a location ~0.2 mm downstream of the nozzle exit. Each spectrum represents the sum of two, 600-second long camera exposures.

In addition to increasing the flow rate and operating with a vertically oriented probe volume, increasing the exposure time has the potential to improve the chances of detecting a Raman signature [16]. Figure 7 presents two measurements made under high-vacuum conditions (~9×10^{-5} Torr) with single-fame exposure times of 30 minutes (middle) and 2 hours (right). Given the challenge of making such long-duration measurements, proper background measurements were not made in this case and thus no background corrections were applied to the results in Fig. 7. However, to demonstrate the similarity between the measurements made with and without gas flowing through the nozzle, the leftmost panel of Fig. 7 displays a spectrum derived from a single 240-second long exposure made in the absence of gas flow. As expected, Fig. 7 demonstrates an increase in total signal with exposure time. Such increase, however, applies to both any Raman signal that might be present and that associated with scattered light not rejected by the notch filter. That is, while the SNR drastically increases with exposure time, the signal-to-background ratio does not change as both increase at the same rate with increased exposure time. With proper background measurements and subsequent removal, increasing the exposure time is likely to improve the quality of the measurements (in terms of SNR); yet, comparisons between the separate spectra in Fig. 7 suggest that drastically increasing exposure time is not likely to provide a viable solution. Thus, the results in Figs. 5-7 seem to indicate that the number density of H_2 molecules at high-vacuum conditions is simply too small to be detected by the spectroscopy system employed here.

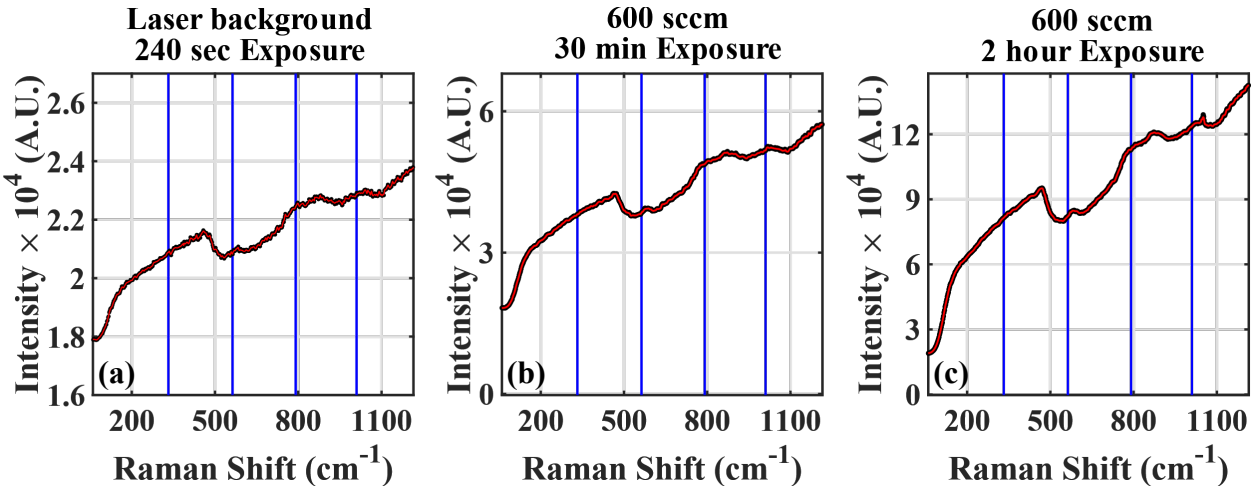

Fig. 7 High-vacuum measurements with varying exposure time durations. (a) Spectrum obtained with no gas flowing from a single 240-second long exposure. (b) Spectrum obtained with gas flowing and from a single 30-minute long exposure. (c) Spectrum obtained with gas flowing and from a single 2-hour long exposure. Note, no background signal was removed from the spectra in panels (b) and (c).

Low-vacuum conditions

To help shed light on why no Raman signal was detected under high-vacuum conditions, measurements were also made at low-vacuum conditions (i.e., chamber pressures between of 0.02 Torr to 4 Torr). Figure 8 presents spectra obtained with 1000 sccm of H_2 flowing through the nozzle and issuing into the chamber with pressures of ~3.6 Torr (left) and ~1.8 Torr (right).

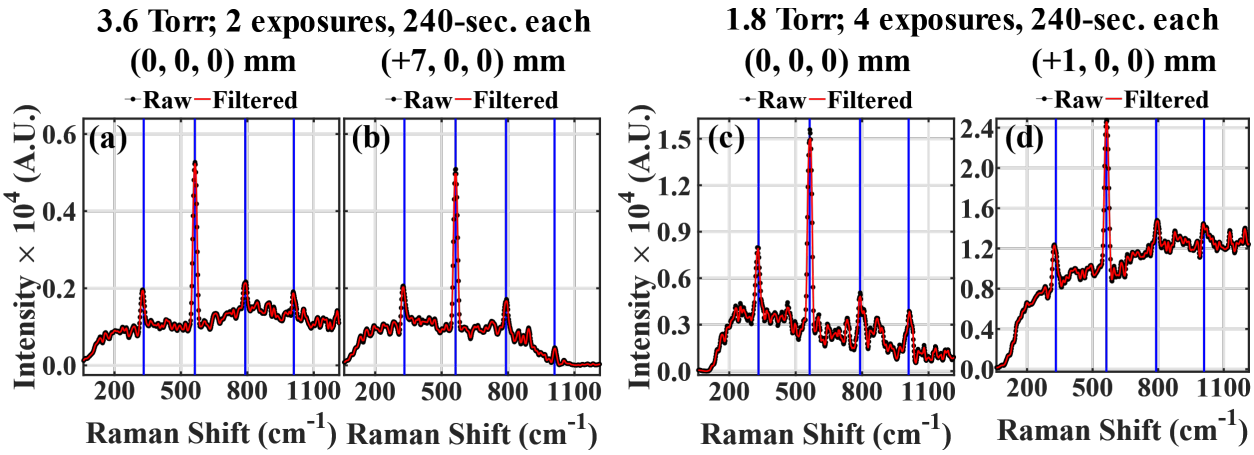

Fig. 8 Low-vacuum measurements made with 1000 sccm of H_2 flowing through the nozzle into a chamber at a pressure of 3.6 Torr in (a) and (b) and 1.8 Torr in (c) and (d). (a) and (b) present the raw and filtered data obtained on centerline and 7-mm off centerline, respectively. (c) and (d) present the raw and filtered data obtained on centerline and 1-mm off centerline, respectively. The spectra in (a) and (b) were derived from two, 240-second exposures, while those in (c) and (d) were produced from four, 240-second exposures.

The spectra in Fig. 8 display strong H_2-Raman signals. Careful inspection of Fig. 8 suggests that the signal-to-background level does not change when the probe volume is moved away from the nozzle to positions where little to no flow is expected. To highlight this observation, Fig. 9 displays sample images

and profiles of the data in Fig. 8 without any background corrections. Additionally, the bottommost row of Fig. 9 presents the difference between the measurement made off- and on-centerline.

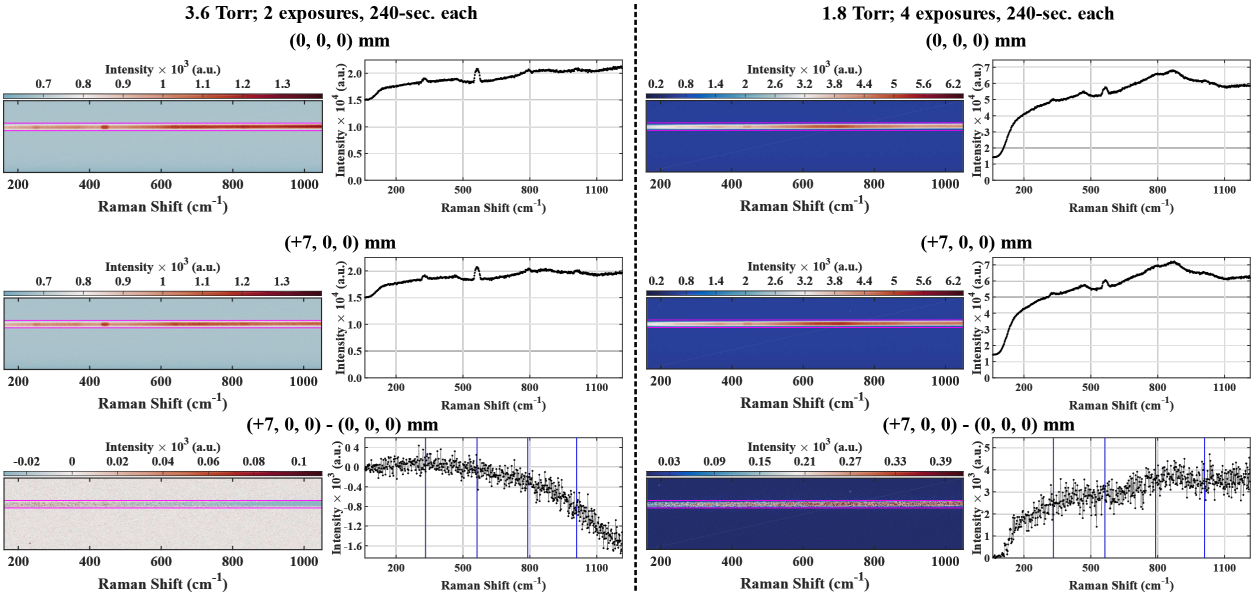

Fig. 9 Sample images and profiles of uncorrected measurements associated with those presented in Fig. 8. The top and middle rows present measurements made along centerline and off centerline, respectively. While the bottom row displays the difference between the latter and the former.

Figure 9, particularly its bottom-most row, clearly demonstrates that there is little to no differences between measurements made on- and off-centerline. Overall, the results in Figs. 8 and 9 imply that, at such large chamber pressures, the diagnostic system employed here is incapable of discerning between Raman signal associated with the H_2 issuing from the jet and that building up within the chamber.

In an attempt to circumvent this issue, measurements were made at chamber pressers of ~0.05 Torr with a large, unmetered amount of H_2 following through the nozzle (i.e., with ~25 psi of pressure upstream of the nozzle throat). Results of such measurements, which were made with the probe volume in a horizontal orientation and were derived from a single 240-second-long exposure, are presented in Fig. 10a. Additionally, Fig. 10b displays spectra obtained with the H_2 heated to 300° C. Yet, even with such large flow rates and a moderate pressure level, no Raman signal is present in the spectra of Fig. 10a. Moreover, it is apparent from Fig. 10b that heating the gas did not provide any improvements.

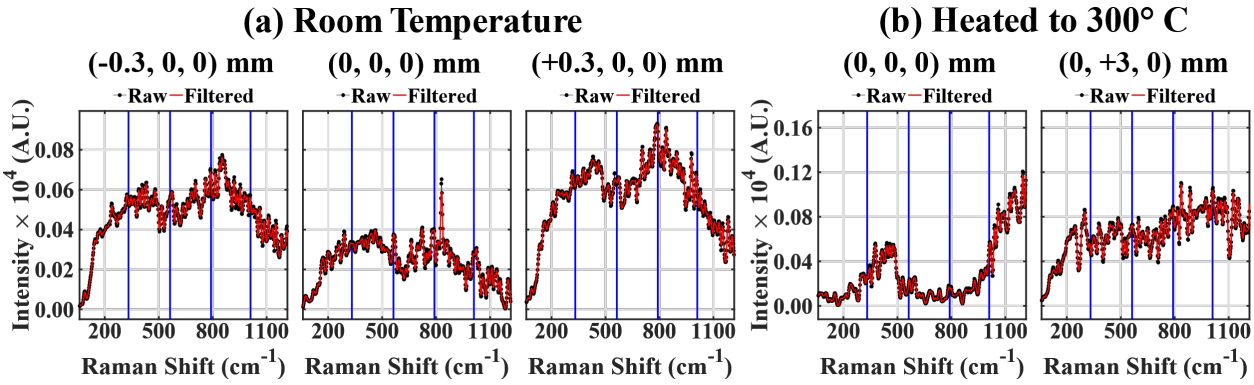

Fig. 10 Low-vacuum measurements made with an unmetered amount of H_2 flowing through the nozzle into the chamber at a pressure of 0.05 Torr. (a) Gas was un-heated. (b) The gas was heated to 300° C.

Though the results in Fig. 10 are void of discernable Raman signal, utilizing the MPC with the probe volume oriented vertically has the potential to increase chances of observing a signal. Figure 11 displays spectra obtained under similar conditions as those associated with Fig. 10a, but with the probe volume oriented vertically. It is clear from Figs. 11a and 11b, which present spectra obtained on and 10 mm above centerline, respectively, that operating with the MPC with a vertical orientation allows for the detection of modest levels of Raman signal. However, as the images and profiles in Fig. 11c (which are similar to those in Fig. 9) indicate, there is no substantial difference between the measurement made on centerline and that made 10 mm away from centerline. Thus, as in the case of the higher-pressure measurements made above, even with the MPC operating with a vertical orientation and with the chamber pressure set relatively low, the spectrometer system utilized here is incapable of distinguishing between Raman signal originating from the jet and that merely associated with background H_2.

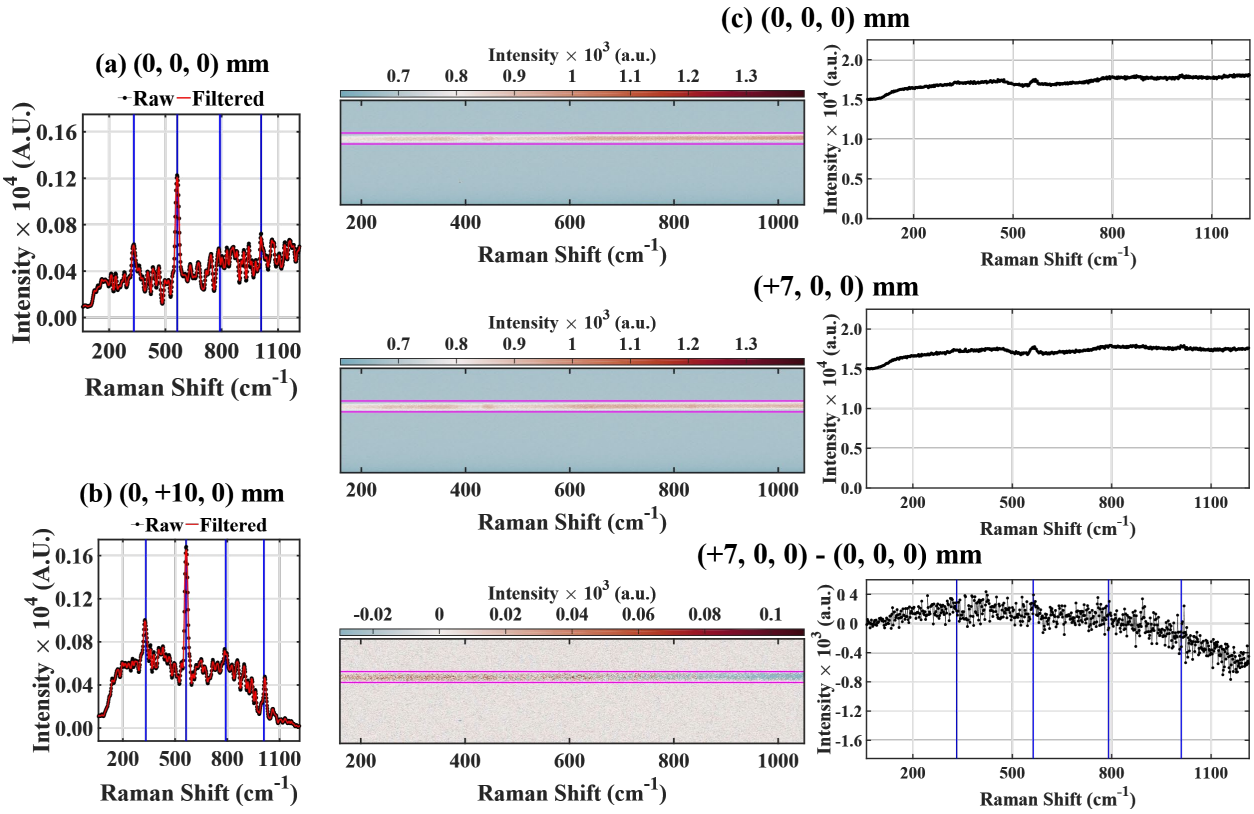

Fig. 11 Low-vacuum measurements (chamber pressure of 0.07 Torr) with a large, unmetered flow of H2 through the nozzle and with the probe volume oriented vertically.

Background removal issues

One consistent feature of the spectra presented above is a non-zero offset to their baseline. That is, even after subtracting background fields (made without gas flowing but with the laser on) from the measurements, a background signal typically remained. Moreover, as is evident from plots above (see Fig. 8, in particular), the background signal level appears to depend on where the measurement was made. Also, close inspection of the raw data (not shown here) suggest that the level of background signal would vary in time.

Figure 12 serves to highlight the severity of this issue by considering theoretical fits to the spectra in Figs. 8a and 8b. Namely, Figs. 12a and 12c plot the same spectra in Figs. 8a and 8b, respectively, while Figs. 12b and 12d present plots with theoretical fits to the filtered data. Additionally, the temperatures associated with these best-fits are provided in red. While the signal in Fig. 12 is strong enough to facilitate the least-squares fitting routine outlined in Ref. [16], the temperature values resulting from this process are not correct as the gas was near room temperature and no heating or cooling was applied. The failure of the fitting routine to provide accurate temperature results here appears to be linked to the non-zero offset of the baseline of the spectra in Fig. 12. Specifically, without a near-zero background (or one that is significantly lower than the Raman signal), the theoretical spectrum is fit in a manner that gives improper weighting to the various rotational transitions, resulting in an erroneous temperature estimate. Note, since the background signal varies with wavenumber, simply removing an additional constant from the data will not suffice. For example, removing an additional constant from the data in Fig. 12d to eliminate the background signal would also remove all of the signal associated with the $S_{J=3}$ transition. Obviously, such modifications would also negatively impact the temperature estimates.

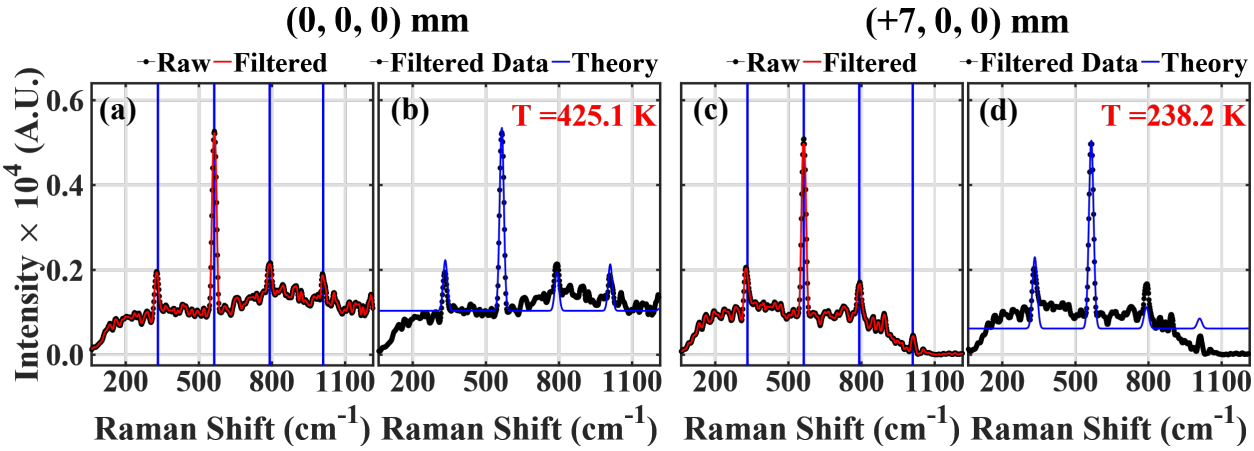

Fig. 12 Low-vacuum measurements made with 1000 sccm of H_2 flowing through the nozzle into a chamber with a pressure of 3.6 Torr. (a) and (c) present the raw and filtered data obtained on centerline and 7-mm off centerline, respectively. (b) and (d) presented the filtered data (black) from (a) and (c), respectively, with the theoretical fit (blue) overlaid. The temperatures in panels (b) and (d) are associated with the best fit to the data. Note that proper background subtraction was employed.

The above assessment indicates that great care must be taken to properly account for the background signal associated with the diagnostic system utilized here. For instance, if meaningful Raman signals can be detected with this system, background measurements should be made immediately before and after those with gas flowing through the nozzle. Additionally, all possible approaches to minimizing the background level without affecting the Raman signal should be considered and implemented.

CONCLUSIONS

This report presents spontaneous Raman scattering measurements made in the exhaust plume issuing from a micro-thruster operated within a vacuum chamber. A novel fiber-coupled, multiple-pass cell (MPC), spontaneous Raman scattering spectroscopy system was employed to facilitate measurements of rotational Raman signals of H_2 gas flowing through the nozzle. Two chamber pressure conditions were considered: High-vacuum (3×10^{-5} Torr and 2×10^{-4} Torr) and low-vacuum (0.05 Torr and 4 Torr). Additionally, measurements were made with the probe volume of the MPC oriented horizontally and vertically, where the former and latter provide the best spatial resolution and signal levels, respectively.

The results of these efforts indicate that the highly sensitive Raman scattering spectroscopy system utilized here is insufficient for accurately detecting Raman signals under conditions relevant to micro-thrusters. Specifically, regardless of how the MPC was oriented or how long the sensor was exposed for, no discernable signal was detected when the thruster was operated within a high-vacuum environment. In contrast, at the highest chamber pressures considered (i.e., ~3.6 Torr), relatively strong Raman signals were measured. Yet, the intensity of these signals was found to be independent of measurement location, implying that the spectroscopy system utilized here could not discern Raman signals associated with the H_2 issuing from the nozzle and that built up in the chamber. These findings indicate that modifications to the spectroscopy system employed here are required if it is to be used for accurate measurements under conditions relevant to micro-thrusters. Suggestions for such modifications are provided in the following section.

A secondary observation from these efforts was that proper treatment of background signal is not trivial and yet it is crucial for accurately estimating temperature from the measured Raman signal. Namely, even after background subtractions, a non-zero baseline signal persisted in the Raman spectra. Attempts to

fit theoretical spectra to such data resulted in erroneously large or small temperature values. Thus, in addition to the modifications suggested below, to render measurements with the present diagnostic system accurate and quantitative, great care must be implemented to minimize and properly account for any background signal that reaches the detector.

FUTURE WORK

If nothing else, the work presented here demonstrates that changes to the experiment are necessary if accurate temperature measurements are to be made in the exhaust plume of the micro-thruster. Suggested changes and the rationale for them are listed below. Additionally, the prospect of using separate diagnostic techniques, instead of spontaneous Raman spectroscopy, are also discussed.

Suggested modifications to Raman spectroscopy system:

1. If a fiber-coupled system is utilized, a pick-off line for monitoring the injection of the laser into the fiber should be added just after the point where the laser enters the fiber. This would permit *in-situ* monitoring of the laser throughput and provide an assessment of how well it is launched into the fiber, both of which are critical for minimizing the potential for damaging the fiber.

2. Increase the size of the mirrors used in the MPC and the size of the collection optics. Increasing the size of the mirrors would likely increase the number of passes contributing to the signal, while increasing the size of the collection optics would permit more of the signal to be collected. This, of course, comes at a significant increase in cost and complexity as optics and optical mounts larger than 2 inches are typically not commercially available.

3. Increase the laser power. This would lead to increased signal; however, it is a costly option and would likely require more durable fibers to withstand and transmit the larger power. Additionally, with this approach care would need to be taken to ensure photoionization of the gas is avoided.

4. If possible, avoid fiber coupling altogether. Nearly half of the laser power is lost when fiber coupling, as is the collected signal. Thus, a factor of ~4 in signal stands to be gained by avoiding the use of fibers. Of course, this would likely require significant modifications to the vacuum chamber and/or the design of an isolation system to allow either the laser or spectrometer to be mounted within the chamber.

5. Let the optical system stay fixed and mount the thruster on a transitional stage. This would ensure the MPC does not become misaligned when moving the probe volume to a different location (since the MPC would remain fixed in this configuration). The downside to this, however, is that it would hinder the ability to make Raman measurements simultaneously with thrust measurements.

6. Attempt measurements with nozzles of different sizes and geometries. Starting with a larger nozzle and progressively shrinking its size may increase the chances of discerning between Raman signal from the jet flow and that from the built up H_2 in the chamber.

7. Add a close-circuit camera to monitor the MPC during operation. This would help ensure the cell remains aligned during the measurements. Moreover, one could even include motorized mirror mounts that could be adjusted remotely to re-align the MPC if its alignment were compromised. This may also help position the probe volume with respect to the exit of the nozzle.

As mentioned, instead of modifying the experiment to try and facilitate spontaneous Raman scattering measurements, different diagnostic techniques may prove to be more fruitful. One such technique is CARS, which has been employed previously to measure properties of exhaust plumes issuing from a resistojet nozzle [7,15]. Furthermore, significant advances in CARS techniques have been achieved since those studies [22]. Recent studies have also demonstrated the ability to make CARS measurements with a fiber-coupled delivery and return system [23]. The downside to CARS, however, is that it requires a far more complicated optical setup as well as a much larger spatial footprint for the necessary lasers. Additionally, the cost of an advanced CARS system is likely much greater than that of the Raman system employed here.

ACKNOWLEDGMENT

The authors would like to thank the Office of Naval Research for financial support under the Naval Research Laboratory (NRL) Base Program. A.W. Skiba held a Postdoctoral Fellowship position through the American Society for Engineering Education.

REFERENCES

[1]L. T. Williams, M. S. McDonald, and M. F. Osborn, "Performance characterization of a low Reynolds number micro-nozzle flow," *Proceedings of the 51st AIAA Joint Propulsion Conference*, Orlando, FL, July 2015.

[2]M. F. Osborn, T. D. Homan, D. A. Rosenberg, and S. G. Tuttle, "Overcoming low nozzle efficiency: A test-correlated numerical investigation of low Reynolds number micro-nozzle flow," AIAA-2015-3925. *Proceedings of the 51st AIAA Joint Propulsion Conference*, Orlando, FL, July 2015

[3]L. T. Williams, M. S. McDonald, and M. F. Osborn, "Performance and vibration characterization of a low-thrust torsional thrust balance," (International Electric Propulsion Conference, Atlanta, 2017).

[4]L. T. Williams and M. F. Osborn, "Performance impacts of geometry and operating conditions on a low Reynolds number micro-nozzle flow," (International Electric Propulsion Conference, Atlanta, 2017).

[5]Bayt, Robert L. and Breuer, Kenneth S., "Viscous Effects in Supersonic MEMS-Fabricated Micronozzles," *Proceedings of the 3rd ASME Microfluids Symposium*, Anaheim, CA, November 1998

[6]T. D. Holman and M. F. Osborn, "Numerical optimization of micro-nozzle geometries for low Reynolds number resistojets," AIAA (2015).

[7]I. D. Boyd, D. B. VanGilder, and E. J. Beiting, "Computational and experimental investigations of rarefied flows in small nozzles," AIAA J. **34**, 2320–2326 (1996).

[8]I. D. Boyd, D. R. Beattie, and M. A. Cappelli, "Numerial and experimental investigations of low-density supersonic jets of hydrogen," J. Fluid Mech. pp. 41–67 (1994).

[9]A. Cervone, A. Mancas, and B. Zandbergen, "Conceptual design of a low-pressure micro-resistojet based on a sublimating solid propellant," Acta Astronaut. **108**, 30–39 (2015).

[10]D. C. Guerrieri, M. A. C. Silva, A. Cervone, and E. Gill, "An analylitical model for characterizing the thrust performance of a low-pressure micro-resistojet," Acta Astronaut. **152**, 719–726 (2018).

[11]R. H. Lee, T. C. Lilly, E. P. Muntz, and A. D. Ketsdever, "Free molecule micro-resistojet: Nanosatellite propulsion," Tech. rep., Air Force Research Laboratory, Edwards AFB (2005).

[12]Z. Ahmed, S. F. Gimelshein, and A. D. Ketsdever, "Numerical analysis of free-molecule microresistorjet performance," J. Propuls. Power **22** (2006).

[13]M. M. Hussaini and J. J. Korte, "Investigation of low-reynolds-number rocket nozzle design using pns-based optimization procedure," Tech. rep., NASA Technical Memorandum, Hampton, Hampton (1996).

[14]G. J. Williams, J. J. Kojima, L. A. Arrington, M. C. Deans, B. D. Reed, M. I. Kinzbach, and C. H. McLean, "Plume characterization of a laboratory model 22n gpim thruster via high-frequency Raman spectroscopy," (AIAA, Orlando, 2015).

[15]E. J. Beiting, "Coherent anti-stokes Raman scattering velocity and translational temperature measurements in resistojets," Appl. Opt. **36** (1997).

[16]A. D. Tuesta, B. T. Fisher, A. W. Skiba, L. T. Williams, M. F. Osborn, "Low Pressure Multiple-pass Raman Spectrometer," *submitted to Appl. Opt*.

[17]K. C. Utsav, J. A. Silver, D. C. Hovde, and P. L. Varghese, "Improved multiple-pass Raman spectrometer," Appl. Opt. pp. 4805–4816 (2011).

[18]K. C. Utsav and P. L. Varghese, "Accurate temperature measurements in flames with high spatial resolution using stokes Raman scattering from nitrogen in a multiple-pass cell," Appl. Opt. **52**, 5007–5021 (2013).

[19]R. A. Hill and D. L. Hartley, "Focused, multiple-pass cell for Raman scattering," Appl. Opt. pp. 186–192 (1974).

[20]R. Trutna and R. L. Byer, "Multiple-pass Raman gain cell," Appl. Opt. pp. 301–312 (1980).

[21]A. C. Eckbreth, Laser Diagnostics for Combustion Temperature and Species (CRC Press, 1996).

[22]S. Roy, J.R. Gord, A.K. Patnaik, Prog. Energy Combust. Sci. 36 (2010) 280–306.

[23]K. Frederickson, S.P. Kearney, A. Luketa, J.C. Hewson, T.W. Grasser, K. Frederickson, S.P. Kearney, A. Luketa, J.C. Hewson, K. Frederickson, S.P. Kearney, A. Luketa, J.C. Hewson, T.W. Grasser, Combust. Sci. Technol. (2010) 941–959.